Sensors & Transducers, Vol. 269, Issue 2, July 2025, pp. 62-70

www.sensorsportal.com

Sensors & Transducers

Published by IFSA Publishing, S. L., 2025
http://www.sensorsportal.com

Multi Slits Interference Test Experiments for Analog Computing

[1,2,*] Dmitry Tsipenyuk, [2] Valery Slobodyanin, [3] Andrey Voropinov, [2] Konstantin Sevastianov, [2] Ilya Krivtsov and [2] Maria Smirnova

[1] All-Russian Institute of Scientific and Technical Information of the Russian Academy of Sciences, Moscow 125190, Russia
[2] Moscow Institute of Physics and Technology, Moscow Region, 141701, Russia
[3] LaserGraphicArt Ltd, Moscow, 105318, Russia
E-mail: Dimat777@list.ru, Slobodyanin.v@mail.ru, avv@lasergraphicart.com, sevastianov.kk@phystech.edu, krivtsov.ia@phystech.edu, smirnova.ma@phystech.edu

Received: 13 April 2025 Revised: 30 June 2025 Accepted: 17 July 2025 Published:25 July 2025

Abstract: Optical computing is a promising area of modern science and technology. Optical computing logical elements could be based on the different optoelectronic techniques or optical space modulators. One of the possible techniques for optical computing is using multi-slit interference. The accuracy of various optical experiments was hampered by the difficulty of making appropriate narrow slits for 2- or 3-slit diffraction experiments. The solution to these and similar technical difficulties could be to alter the radiation spectrum from the classical optical range in the microwave region. In the present paper, we present preliminary two- and three-slit interference microwave test experiments. For the interference, we used different metal coatings with two and three slits with different widths. Diffraction experiments were done for the 37.3 and 48.3 GHz microwave frequencies. We could investigate possibilities to manage microwave two- and three-slit interference by changing microwave polarization and introducing a time delay in the microwave path. During the investigation, we seek quantum effects in the near Fresnel zone and far Fraunhofer zones. This paper investigates the feasibility of modeling wave scattering on various volumetric objects (microwave transducers) using a physically based neural network approach also.

Keywords: Diffraction, Interference, Multiple-slit experiments, Microwave photonics, Photonic computing, Microwave wavefront transducer.

1. Introduction

Modern optics has a fundamental contradiction that is rarely talked about. The quantization and transmission of photon energy as a fraction (an energy quantum) is one side. In contrast, the Huygens-Fresnel principle asserts that a radiation wave (a photon) can be split into a variety of secondary sources (waves). Adding these secondary waves allows for the description of any optical phenomenon, including diffraction and interference.

Obviously, the Huygens-Fresnel principle is a mathematical method or technique. Experimental verification is necessary for basic postulates like the splitting of a photon into parts and their integration into total energy in physics, which is an experimental science.

The only thing we are certain about today is that one photon can pass through two slits at once. By splitting the photon into two parts, the resulting diffraction image is highly influenced by the observer's behavior.

Naturally, conducting comparable experiments in the microwave range is significantly simpler, and a few of our initial findings are showcased here.

The challenges associated with investigating diffraction and interference, particularly in the Fresnel zone when dealing with small slit dimensions, stem solely from technical difficulties. These arise from the difficulties involved in precisely observing the

diffraction characteristics at reduced sizes of the diffraction pattern within the optical spectrum, such as for visible light (ranging from 380 nm to 760 nm), and the complication of creating and effectively managing the relevant slits.

One potential solution to this issue involves extending the operational wavelength into the microwave frequency band. Preliminary findings from investigations into diffraction and interference phenomena within the microwave range are detailed subsequently.

On the basis of photonic interference, it is possible to elaborate interference-based logic gates [1] and develop different types of photonic integrated circuits [2]. Some patents and technology solutions concerning optic computing can be found at [3-7].

The investigation potentially could provide new tools for controlling multiphoton interference; this may help researchers to design new tests of optical computing and probability quantum mechanics, optical-communication protocols, and quantum simulators.

2. Experimental

A brief description of the experimental setup installation can be found in references [8-9]. The microwave generator (G4-141) operates at a frequency of 38 GHz, with a range of 36.5 to 53.5 GHz. The output signal power is adjustable from 1 to 0.004 W, and the power level can vary by 30 dB. The output frequency exhibits stability within ±0.001 GHz.

After the microwave generator, the radiation propagates along a silver-plated copper waveguide with a length of 23.0 mm and a rectangular cross-section (a×b = 5.5×2.5 mm). A more detailed description of the experimental setup and test measurement results can be found in references [8, 11].

The installation includes an output horn antenna with a diameter of 45 mm and a length of 75 mm, as well as a waveguide with a wall thickness of 1.2 mm made of copper and silver-plated on the inside.

The receiving device, equipped with a horn antenna measuring 35 mm in diameter and 55 mm in length, can be moved precisely (with an accuracy of 0.1 mm) across three dimensions within a range of 0 to 140 mm thanks to its integrated three-dimensional positioning system. The received microwave signal undergoes analog-to-digital conversion (ADC) before being relayed to a central control computer for processing.to a central control computer for processing.

The installation diagram was shown in Fig. 1. Microwave radiation with a frequency of 38 GHz was generated by generator 1 of brand G4-141 (main generation range 36.0-54.0 GHz) or G4-142 (main generation range 54.0-79.0 GHz). The output signal power is adjustable from 1 to $4 \cdot 10^{-3}$ W, the range of the output power level is 30 dB. The output frequency instability in time does not exceed 10^{-3}. The limit of instability of the output power level is ± 0.3 dB. After the microwave generator, the radiation propagates along a silver-plated copper output waveguide of 23.0 mm length and rectangular cross-section a×b = 5.5×2.5 mm.

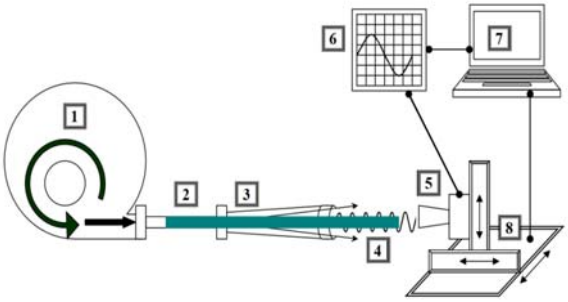

Fig. 1. Scheme of the installation. 1 - microwave generator 36-79 GHz, 2 - rectangular waveguide, 3 - output horn/sectoral antenna, 4 - Teflon or silicone dielectric insert of variable cross-section, 5 - microwave receiver, 6 - digital oscilloscope, 7 - computer, 8 - receiver 3D positioning system.

The installation can accommodate a horn antenna 3 (output diameter 45 mm and length 75 mm) and a waveguide 2 with a wall thickness of 1.2 mm, made of copper and silver-plated on the inside.

The receiver 6 combined with a horn antenna (input diameter 35 mm, length 55 mm) can be moved precisely in three spatial directions (movement accuracy 0.1 mm in the range 0-140 mm) using the three-dimensional positioning system of the receiver 7. The microwave signal received by the receiver is processed by the ADC and then transmitted to the control computer.

Fig. 2 shows the results of measuring the shape of the microwave wave vertical profiles with at a frequency of 38 GHz emitted from a rectangular waveguide with a cross-section of 5.5×2.5 mm, combined with an output horn with a diameter of 45 mm and a horn length of 60 mm.

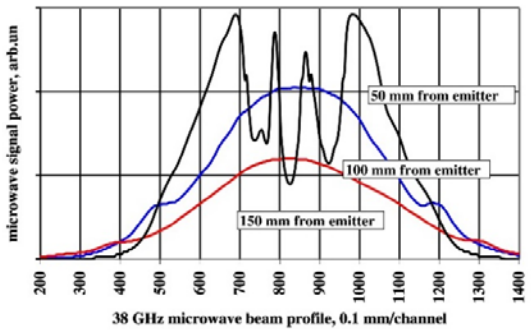

Fig. 2. Comparison of the shape of the 38 GHz microwave beam profile (without taking into account the relative magnitude of the signal), depending on the distance from the transmitter to the receiver 50 mm - Fresnel region; and Fraunhofer region - 100- and 150-mm. Output horn diameter 45 mm, horn length 60 mm and input horn diameter 35 mm, horn length 50 mm.

Vertical profiles were measured both at the centre of the beam in the horizontal direction and with detuning every 5-10 mm from the centre. As shown in Fig. 2, vertical waveforms were measured at different distances of 50, 100 and 150 mm from the beam. Fig. 2 shows the shape of the waveform at different distances without taking into account the real value of the received signal. It can be seen that at a distance of 50 mm the wave has not yet fully formed, which corresponds to the near Frenel diffraction zone for radiation at a frequency of 38 GHz (wavelength 7.89 mm). At a distance of 100 mm, the wavefront is practically formed, corresponding to the far Fraunhofer diffraction zone.

At the Fig. 3 shows the change in the signal with a linear shift of the receiver along the direction of propagation of the microwave signal by 50 mm.

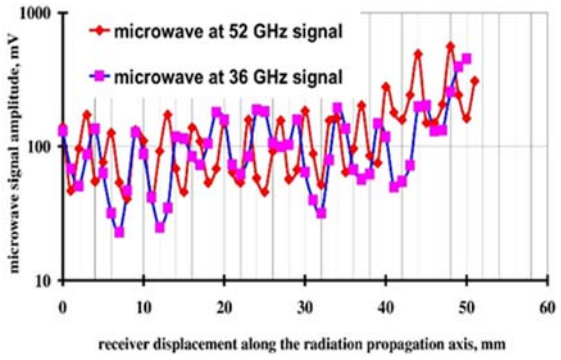

Fig. 3. The structure of standing waves generated in the waveguide connected to the receiver input when the receiver is moved towards the emitter by 0-51 mm. The measurements were carried out at two radiation frequencies of 36.0 and 52.0 GHz.

The frequency of the transmitter in two measurement series of measurements was 36.0 and 52.0 GHz, the current set on the output power regulator was 70 mA, which corresponds to the maximum output power (Fig. 3). The measurement accuracy of the microwave amplitude in this signal series was 0.1-0.2 mV.

The number of periods of stationary microwave waves established in the receiving waveguide is proportional to the frequencies of the initial radiation: the ratio of the initial frequencies 52.0/36.0 = 1.44 coincides (Fig. 3). Taking into account the accuracy of the measurements, with the ratio of the number of periods measured when the receiver is moved to a length of 51 mm 16/11 = 1.45.

These results are in good agreement with theoretical ideas about the formation of a wavefront during the emission of electromagnetic radiation, depending on the distance along the direction of radiation propagation.

This study describes 2-3-4 slit interference experiments carried out at different distances between the emitter and the slits, encompassing both the Fresnel and Fraunhofer regions. The results will be compared with computer simulations using various programs, including Fresnel [12] and CST STUDIO SUITE [13]. The study will also consider the potential use of electrodynamic modeling and design systems such as HFSS (High Frequency Structure Simulator), IE3D, Microwave Office, and Microwave Studio. A comparison with three-slit experiments in the microwave and optical regions [14-16] will also be made. This work investigates the feasibility of modeling wave scattering on various volumetric objects (microwave transducers) using a physically based neural network approach.

At Fig. 4a, a 3-slit (each 8.0 mm wide, 130 mm high, and 8.0 mm between slits) sample construction was presented, which was used for our interference experiments. The base of construction was made from plastic 2.0 mm wide and coated with the 0.1 mm aluminum film from one side.

At the Fig. 4b, the full plastic construction, which supports a changeable slits plate, is presented.

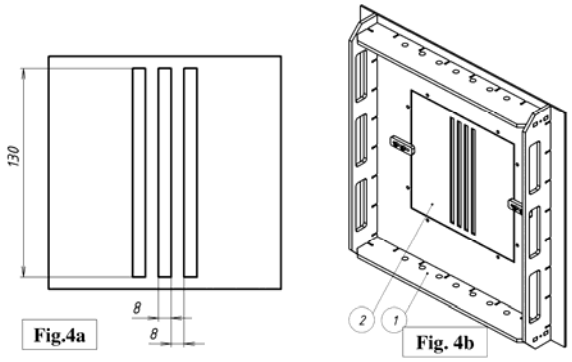

Fig. 4 (a). A sample of an interchangeable set of 2 or 3 metallized slits (widths from 3 to 10 mm.); (**b)** Mounting structure for securing replaceable sets of slots.

In this paper, we present results of horizontal profile interference measurements using two and three slits, each 10.0 mm wide and 130 mm high. The distance between slit centers was 32.0 mm for the two-slit sample and 17.0 mm for the three-slit sample.

An interchangeable set of 2 or 3 slits 10.0 mm wide was placed between the output horn/sectoral antenna and the microwave receiver. The distance in the center of the microwave wave from the output horn and slits was 100.0 mm, and the distance from the slits to the receiver was 110.0 mm.

We also conducted experiments with distances of 150 mm from the output horn to the slits and 120-150 mm from the slits to the receiver.

We investigated horizontal interference profiles at the center of the beam. Interference profiles were measured primarily for frequencies of 38.3 and 48.3 GHz.

3. Experimental Microwave Results

The results presented below made with the same experimental geometry wave and frequency of 48.3 GHz, 150 mm from the source up to the slits, and 120 mm from the slits up to the receiver, with a horizontal profile of 140 mm in length.

Fig. 5, presented: geometrical profile of two slits 10 mm wide and 37 mm between the center of the slits and microwave 48.3 GHz beam profiles when only the left or right slit was open.

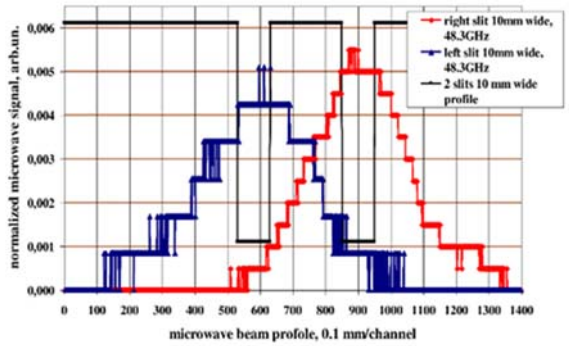

Fig. 5. Microwave horizontal beam profiles at 48.3 GHz when only the left or right slit is open and geometrical profile of two slits 10 mm wide overlapping at the single beam slit profiles.

Interference beam profile from 2-slits 10 mm wide presented in Fig. 6. In addition to the 2-slits interference geometrical profile of the slits, was add at Fig. 6.

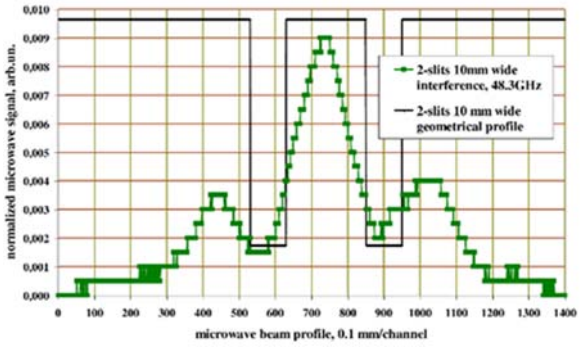

Fig. 6. Microwave beam profiles at 48.3 GHz when both left and right slits were open and geometrical profile of two slits 10 mm wide overlapping at the single beam slits profiles.

As we can see, beam center profiles of the single slit approximately coincide with the geometrical slit profile (Fig. 5), and beam profiles from 2-slits have a minimum in the geometrical 2-slits profile (Fig. 6).

We would like to mention that interference profile from fully dielectrical set of slits is the same.

We investigate possibilities to manage the 2-slits diffraction profile by introducing a time delay between the optical signals from the slits. For this purpose, we establish dielectric plastic 2 to 18 mm wide in front of one of the two slits.

At the Fig. 7, we present summary results of introducing 2-4-6-8-10 mm plastic thicknesses into the right slit.

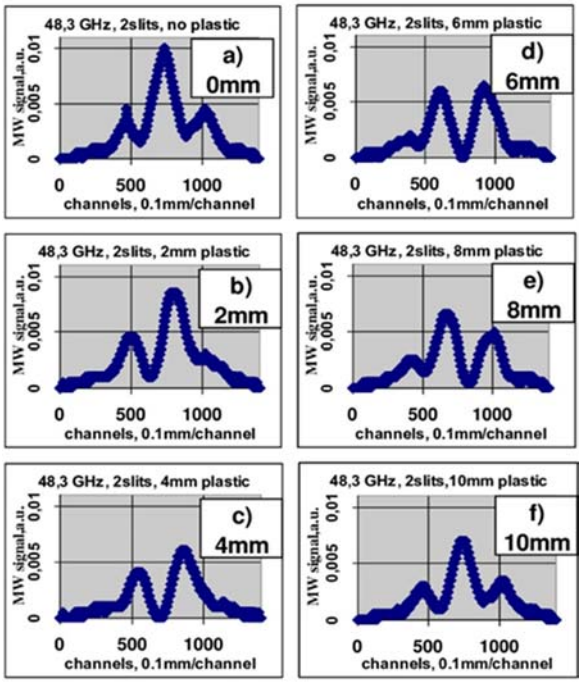

Fig. 7. Microwave beam profiles at 48.3 GHz from 2-slits 10 mm wide. Profiles a)-b)-c)-d)-e)-f) appropriate to dielectric plastic 0-2-4-6-8-10 mm thicknesses in the right slit.

As we can see, microwave interference profiles shape without plastic in the right slit Fig. 7a coincide with profiles with 10 mm plastic in the right slit Fig. 7f. This means that the time delay between 7a) and 7f) equals 2π shift, while the microwave signal amplitude diminished about 1.4 times due to microwave dielectric plastic absorption.

For the 3-slits interference experiments, we obtain similar but more complex beam profiles. Nevertheless, we can clearly distinguish different sets of 3-slits interference in all cases when we manage microwave time delays in any of the three slits.

We could change the interference beam profiles from 2 and 3 slits by introducing wave time delays and polarization in different slits.

At the Fig. 8 horizontal microwave beam profiles present for the one slit 6mm wide and microwave frequencies 38.4, 48.5 and 59.2 GHz.

We measure horizontal wave profile in the case when the distance between emitter was 70 mm and slits slot and the distance between slit slot and receiver was 70 mm also for the Fig. 8-11.

As shown in Fig. 8, microwave beam profiles after a 6.0 mm slit yield drastically different results for frequencies of 38.4 GHz, 48.5 GHz and 59.2 GHz. This difference is not evident when considering that the wavelengths corresponding to these frequencies

are 7.81 mm (38.4 GHz), 6.18 mm (48.5 GHz), and 5.06 mm (59.2 GHz).

We have a design with interchangeable set of 2-3-4 slits of various widths 3, 4, 5, 6 and 8 mm.

Any size slits set was placed between 3 - output horn/sectoral antenna and 5 - microwave receiver at the Fig. 1.

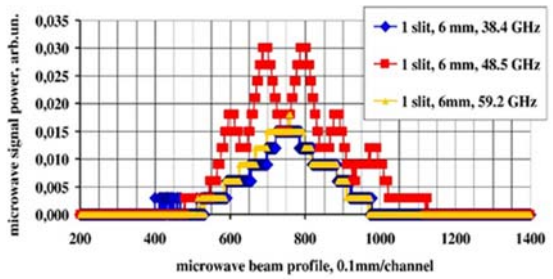

Fig. 8. Microwave beam profiles (38.4; 48.5 and 59.2 GHz) from one slit 6 mm wide at the distance 70 mm from the slit.

Fig. 9 shows similar results to Fig. 10, when different microwave wavelengths produce different beam profiles from the same sets of three-four 6-8-mm-wide slits set.

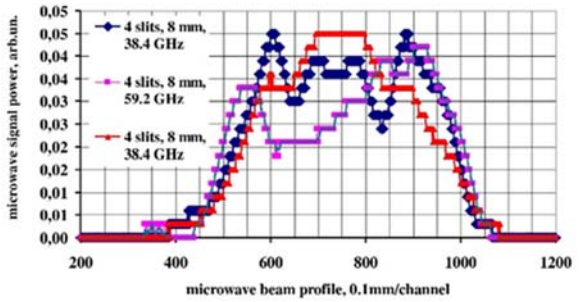

Fig. 9. Microwave beam profiles (38.4; 48.5 and 59.2 GHz) from three slits 8 mm wide at the distance 70 mm from the slits slot.

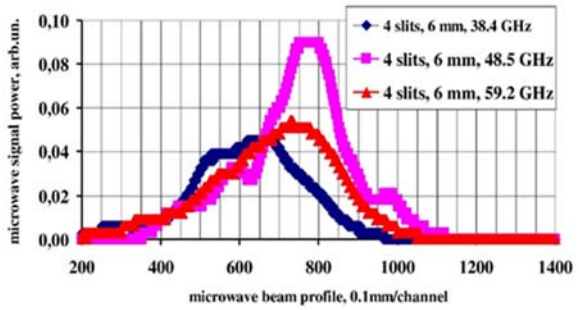

Fig. 10. Microwave beam profiles (38.4; 48.5 and 59.2 GHz) from four slits 6 mm wide at the distance 70 mm from the slits slot.

Fig. 10 presents wave profiles from four slits, each 6 mm wide. The difference between the results in Fig. 9 and Fig. 10 is due to our use of a 6.0 mm slit (Fig. 10) instead of an 8.0 mm slit (Fig. 9).

Fig. 11 shows the wave profile for the same microwave wavelengths (38.4 GHz, 48.5 GHz, and 59.2 GHz). The difference between Fig. 11 and Fig. 10 is that only three out of four slits (each 6 mm wide) are open. Looking at the slit set from left to right, the first two slits are open, the third slit is closed, and the fourth slit is open.

As shown in Fig. 11, we can easily distinguish all three different waves from the beam profile. The 38.4 GHz beam exhibits three widely situated maxima; the 48.4 GHz beam shows three narrowly situated maxima; and the 59.2 GHz beam displays only two (or three?) wide main maxima. It is interesting to compare Fig. 11 and Fig. 8 results also.

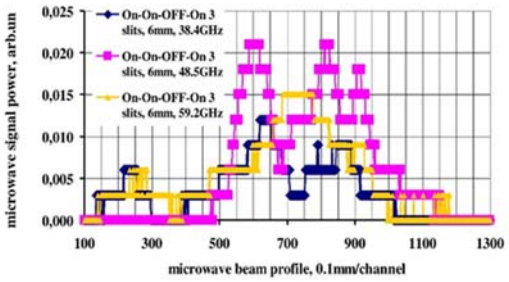

Fig. 11. Microwave beam profiles (38.4; 48.5 and 59.2 GHz) from three slits 6 mm wide at the distance 70 mm from the slits slot. The slits slot had geometry from the left to the right: two slits are open, the one slit was closed and the last slit was open.

From our perspective, the method used in this paper enables a more accurate experimental study of diffraction and interference by shifting the radiation wavelength from the optical range of conventional optics to the microwave range.

We are confident that these changes in the measurement range will not only significantly improve the accuracy of numerous optical measurements but also enable us to perform experiments that are currently difficult to conduct within the optical range. For instance, we will be able to experimentally measure the impedance of empty space (vacuum [17]) for the first time.

5. Interference Experiments in the Optical Field

The other set of slit experiments was done in the optical wave region. The setup diagram and detailed description were presented in [18].

The light source was a semiconductor laser with a wavelength of 450 nm and a spectrum width of 0.7 nm, emitting a continuous sequence of pulses with a frequency of the f = 1 kHz, with an average power of 15 mW and a peak power of 50 mW. The light beam

from this laser was fed to a grid of several slits 50 μm wide Fig. 12.

The use of several slits instead of two, used in the classical Young scheme, facilitates the alignment of the setup, since small transverse displacements of the laser beam (~ 100 μm) do not lead to the disappearance of interference even with a small beam diameter. The laser radiation is slightly focused, so that the laser beam captures 3-4 slits.

The radiation that passes through the grating enters a light-insulated box, in which a photodetector is placed near the opposite wall – a highly sensitive photomultiplier tube with a response time to a single photon of about 10^{-8} s.

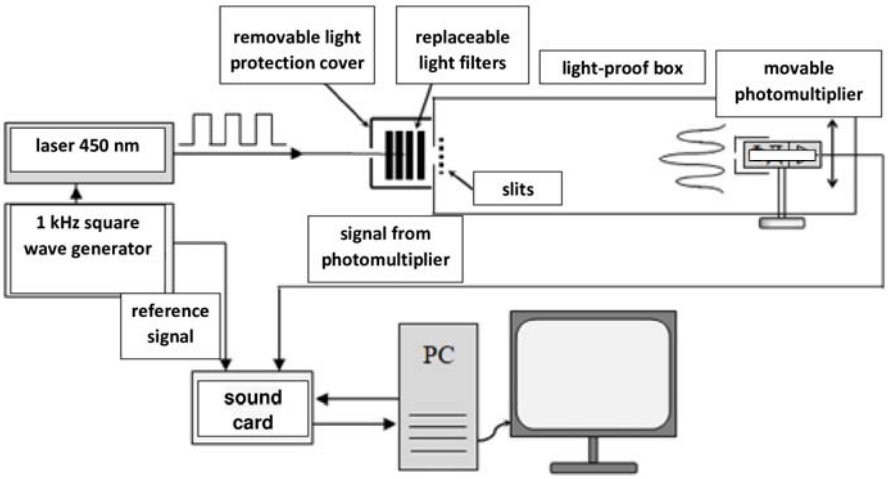

Fig. 12. Optical interference setup diagram. 450 nm laser radiation was passed through a filter holder and entered a light-insulated box. Light was scattered by optical slits and then reached a highly sensitive photomultiplier. The electrical signal from the photomultiplier was registered using the method of synchronous detection, “lock-in amplification”.

The photodetector can move 15 mm from the left to the right in the direction transverse to the light beam.

In front of the slit grid there was a filter holder, into which we could insert the required number of dark glass filters and weaken the beam by the required number of times.

Measurements were carried out with the initial beam weakened by many orders of magnitude, from 10^{-6} up to 10^{-12} times.

In this investigation, we use the method of synchronous detection, "lock-in amplification." It is used for periodic electrical signals and allows us to measure very noisy signals.

In the literature, there are reports of "pulling out" a signal from noise that is 10^7 times weaker than the noise.

We can estimate mean distance between photons in the case of maximum weakening. The transmission of filters T = $2.9*10^{-12}$, therefore the power of the light beam after the filters P =$1.1*10^{-13}$ W, the photon repetition period $\Delta T \approx 1\mu s$, the average distance between photons, if they are hypothetically lined up, $\ell \approx 1.0km$.

In this work, a synchronous detector is used, implemented in software on a personal computer and included in the PhysLab package.

The PhysLab program turns the computer into a measuring center and includes an oscilloscope, a Fourier spectrometer, and a synchronous detector.

The signal from the photodetector is digitized by an external sound card. We use an external Motu M2 USB card, which has much lower noise than the sound cards built into the motherboard. Motu M2 USB card dynamic range is 110 dB.

This means that its own noise is five and a half orders of magnitude lower than the maximum permissible amplified signal.

At the Fig. 12, the set of interference profiles with different light weakening from 10^{-6} up to 10^{-13} presented.

As we can see, there is no sufficient experimental difference in the interference profiles in the case of light in the waveform and in the quantum single-photon interference.

Thus, we would also like to consider the following discussion view on optical and quantum calculation: We found from experimental results that interference beam profiles are the same for multiphoton microwave (or optic) beams and slit single-photon interference experiments.

This gives us possibilities to consider approaches on how to move from quantum to optical calculations.

Such a conclusion is based on our opinion that a simple one slit, which is illuminated by a set of single photons, gives us a diffraction contour that obeys the probability law where a single photon will be reflected after the slit to the left side (50%) or to the right side (50%), and the sum of these probabilities equals 100%. So, one slit could be considered formally as a model of one qubit.

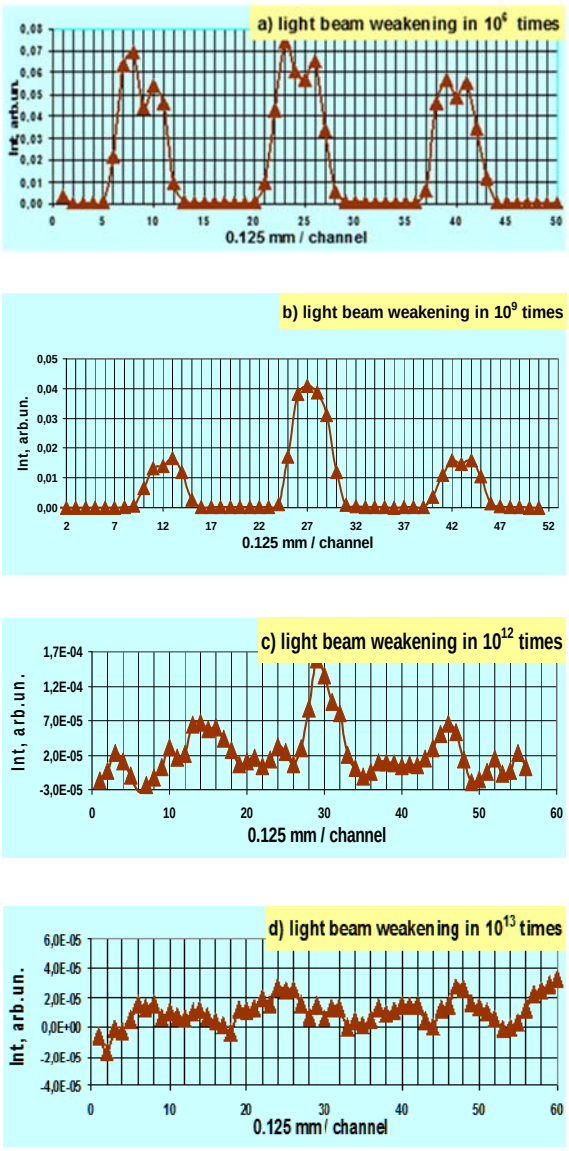

Fig. 12. Interference observation of the rarely following photons, 450 nm, several slits of the 50 μm wide, beam weakening transmission of filters equals: a) T=10-6; b) T=10-9; c) T=10-12; d) T=10-13.

7. Modeling Microwave Scattering from Two Slits

In addition to carrying out interference experiments, we calculate beam profiles for the same slit geometry and wavelength.

Fig. 13 shows the results of calculations of the interference microwave beam profile corresponding to the experimental conditions and experimental results shown at the Fig. 7.

As can be seen, the results of experimental measurements in Fig. 7 and calculations in Fig. 13 qualitatively coincide. As can be seen, the results of the experimental measurements in Fig. 7 and the calculations in Fig. 13 qualitatively coincide. This is clearly seen from the pairwise comparison of variants a-f in Fig. 7 and 13.

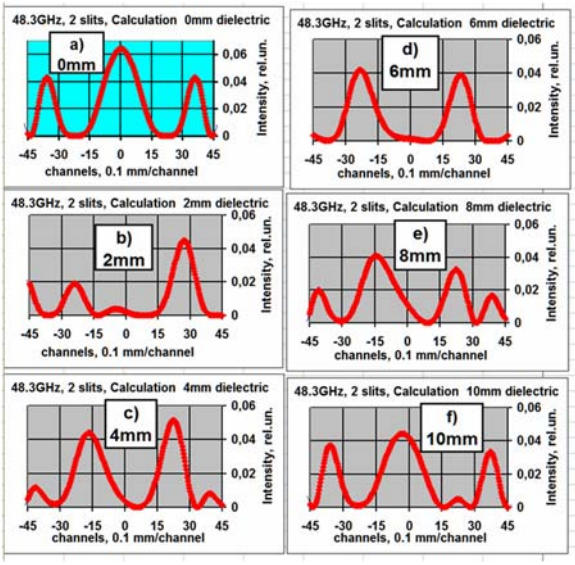

Fig. 13. Calculated microwave beam profiles at 48.3 GHz from two 10 mm-wide slits. Profiles (a)-(f) corresponds to dielectric thicknesses of 0, 2, 4, 6, 8, and 10 mm situated in the left slit.

The calculation model was done at the base of the analysis of the Fresnel diffraction and Mie scattering physics and development at this base numerical scattering simulations using PyMeep Finite-Differences Time Domain (FDTD).

Based on this model, we would like to create an efficient, physically based neural network for optical diffraction tomography.

We can shortly formulate reached calculation results as follows.

An effective model for numerical simulation of electromagnetic wave scattering in a medium has been developed and implemented using the PyMeep library, ensuring high accuracy and scalability of calculations.

An approach has been developed for creating a physically based neural network architecture to restore the distribution of the electromagnetic field. The neural model does not require knowledge of the analytical solution and generalizes the behavior of the field beyond the training sample.

A comparison of computational speed was made. The PyMeep code demonstrates a significant speedup compared to direct numerical calculation of the Fresnel integral, especially on large grid sizes. This confirms the effectiveness of the proposed approach in terms of both accuracy and performance.

We would like to present more detailed descriptions of our calculation model results in future papers.

8. Conclusion

The results demonstrate the possibility of manipulating (transducing) microwave waveforms through optical interference experiments using two, three, or more slits.

We also experimentally show that single-photon interference from the slits does not differ from the wave interference.

At base these experimentally obtained results we could think about optical computing logical sets at the base of the slits interference.

A listing of the minimal requirements for creating a quantum computer was given in [19, 20]:

1) The physical system must be scalable, and the state of the qubits must be known.

A quantum computer must be able to scale up the qubit set to a number sufficient for complex calculations.

A qubit is called "well described" if its properties and interactions with other parts of the system are well known;

2) Another requirement of quantum computation is that it must be possible to place the quantum system in a fiducial starting quantum state;
3) The quantum system to be used as a quantum computer must be to a high degree isolated from coupling to its environment;
4) The system must allow the implementation of a "universal set" of gates.

A universal set of gates is one that is sufficient to perform any quantum computation;

5) The system must support measurement of individual qubits. It must be possible to obtain the result of a computation by reading the final state of individual qubits.

From our point of view, the set of single slits could be considered as qubit construction. The set of such slits eliminated by infrared light or microwave radiation could satisfy 1-5 demands formulated in [19, 20].

There are currently several physical models of quantum computing being actively developed: ion traps, photonic qubits, topological qubits, etc.

Whatever the underlying physical principles, a quantum computer must adhere to the five fundamental principles outlined above.

For example, logic NOR, NAND and XNOR gates based on interference effects were built [21] for possible logical optic calculations in the 1.55 μm region.

Other technical solutions in [1-7] are also considered.

It is well known that classical bits and quantum bits are described by the following mathematics:

A classical bit at any given moment in time can only take on one of two values: 0 or 1.

A classical bit (switcher) can be described as: [1] or [0].

A quantum bit (qubit) obeys the laws of quantum mechanics and can therefore be in a superposition of states 0 and 1. These classical states, 0 and 1 correspond to the Dirac notations $|0\rangle;|1\rangle$.

Qubit state: $|\psi_1\rangle = a|0\rangle + b|1\rangle$. Here a and b are the complex-valued coefficients that meet the normalization requirement $a^2 + b^2 = 1$.

This means that the probability of finding a qubit in one of these two states is 100%, and the probability of finding it in any other state is 0%.

What can this qubit be physically represented by? It could be the electron with its spin (for example, spin up – (1), down – (0), a photon of light with a certain polarization direction, or even a certain direction of particle propagation. In general, everything that can be in a state of superposition.

That is, the state of the qubit is not known before its measurement, and when measured, it goes into one of two possible states. Moreover, the superposition state will be destroyed (here we will get a classical bit of information, depending on the state (0) or (1).

We think that description of light or microwave radiation deflection to the right or left direction after one slit can be described with the same mathematics as a qubit with $a^2=b^2=0.5$.

If the right part will take place 30% and the left part will take 70%, we will have a qubit with another probability distribution of 30/70.

The way to build a real logical system based on the sets of single slits (transducers) in microwave or visible light regions will be the area of our future investigations.

Acknowledgements

Authors would like to reveal thanks for Ruslan M. Sarimov for his help in experiments arrangements.

We would like to thanks Prof. Vladimir A. Petukhov and Prof. Alexander V. Maximychev for the possibility to work at the optical interference installation and for the fruitful mutual discussions.

References

[1]. S. A. Stepanenko, Interference-Based Logic Gates, *Doklady Mathematics*, Vol. 102, Issue 1, 2020, pp. 318–323.

[2]. P. O. Yakushenkov, Photonic integrated circuits, *Photonics Russia*, Vol. 68, Issue 8, 2017, pp. 58–67. (in Russian)

[3]. M. M. Vekshin, V. A. Nikitin, A. V. Nikitin, N. A. Yakovenko, Method for manufacturing of integral microlenses, RF Patent No. 2312833, *Bulletin of Inventions*, No. 35, 2007.

[4]. A. O. Poluektov, An optical logic gate, RF Patent No. 20751061, Published 10 March 1997.

[5]. J.-E. Broquin, Glass integrated optics: State of the art and position toward other technologies, in *Proceedings of SPIE 6475, Integrated Optics: Devices, Materials, and Technologies XI*, 2007, Article 647507.

[6]. M. M. Vekshin, V. A. Nikitin, N. A. Yakovenko, Study and Design of Photonic Integrated Circuits on K-8 Optical Glass Substrates for Functional Data Processing at a Wavelength of 1550 nm, *Optoelectronics Instrumentation and Data Processing*, Vol. 58, 2022, pp. 234–240.

[7]. D. Dai, L. Liu, S. Gao, D.-X. Xu, S. He, Polarization management for silicon photonic integrated circuits,

Laser & Photonics Reviews, Vol. 7, 2013, pp. 303–328.
[8]. D. Yu. Tsipenyuk, A. I. Milanich, V. P. Slobodyanin, A. V. Voropinov, Photons in Two-Three-Four Slits Interference Experiments, in *Proceedings of the 7th International Conference on Optics, Photonics and Lasers (OPAL' 2024)*, Palma de Mallorca, Spain, 15–17 May 2024, pp. 124–128.
[9]. D. Yu. Tsipenyuk, V. P. Slobodyanin, A. V. Voropinov, K. K. Sevastianov, Two and Three Slits Model Interference Experiments for Analog Optical Computing, in *Proceedings of the 8th International Conference on Optics, Photonics and Lasers (OPAL' 2025)*, Rhodes, Greece, 14–16 May 2025, pp. 31–35.
[10]. D. Yu. Tsipenyuk, S. I. Derzhavin, Y. V. Kravchenko, M. R. Bogdanov, Installation for studying the parameters of localization of an electromagnetic wave in a waveguide of variable cross-section in the framework of the predictions of the 5-d extended space model, *RENSIT: Radioelectronics. Nanosystems. Information Technologies*, Vol. 13, Issue 4, 2021, pp. 407–418. (in Russian)
[11]. Y. V. Kravchenko, D. Yu. Tsipenyuk, A. V. Voropinov, Electromagnetic wave localization and scattering parameters investigation in a partially absorbing medium depending on the output tract geometric configuration, *RENSIT: Radioelectronics. Nanosystems. Information Technologies*, Vol. 15, Issue 3, 2023, pp. 205–214. (in Russian)
[12]. I. V. Epatko et al., Inclusion of aberrations of a tilted plane-parallel plate in diffraction calculations of the propagation of radiation, *Quantum Electronics*, Vol. 28, Issue 8, 1998, pp. 703–706. (in Russian)
[13]. *CST Studio Suite*, Electromagnetic Field Simulation Software, available at: https://www.3ds.com
[14]. O. S. Magaña-Loaiza et al., Exotic looped trajectories of photons in three-slit interference, *Nature Communications*, Vol. 7, 2016, Article 13987.
[15]. U. Sinha, C. Couteau, et al., Ruling out multi-order interference in quantum mechanics, *Science*, Vol. 329, 2010, pp. 418–421.
[16]. U. Sinha, C. Couteau, Z. Medendorp, I. Söllner, R. Laflamme, R. Sorkin, Testing Born's Rule in Quantum Mechanics with a Triple Slit Experiment, in *American Institute of Physics Conference Proceedings*, Vol. 1101, 2009, pp. 200–207.
[17]. T. Koryu Ishii, *Handbook of Microwave Technology*, Academic Press, 1995.
[18]. A. V. Maksimychev, V. A. Petukhov, K. K. Sevastianov, Interference Observation of the rarely following photons, in *Proceedings of the 67th MIPT Conference 2025*, Moscow, 31 March – 5 April 2025, *Fizmatkniga* (in press).
[19]. D. P. DiVincenzo, Topics in Quantum Computers, in: L. L. Sohn, L. P. Kouwenhoven, G. Schön (eds), *Mesoscopic Electron Transport*, NATO ASI Series, Springer, Dordrecht, 1997, Vol. 345.
[20]. D. P. DiVincenzo, The physical implementation of quantum computation, *Fortschritte der Physik*, Vol. 48, 2000, pp. 771–779. (in German)
[21]. Sun Xiao-Wen et al., Design and analysis of logic NOR, NAND and XNOR gates based on interference effect, *Quantum Electronics*, Vol. 48, Issue 2, 2018, pp. 178–183. (in Russian)

Published by International Frequency Sensor Association (IFSA) Publishing, S. L., 2025 (http://www.sensorsportal.com).